# ANISOTROPY BASED SEEDING FOR HYPERSTREAMLINE

Wei Shen and Alex Pang
Computer Science Department
University of California
Santa Cruz, CA 95064, USA
email: weishen, pang@cse.ucsc.edu

**ABSTRACT**

This paper presents a new seeding strategy for visualizing 3D symmetric tensor data using hyperstreamlines. The goal is to automate the process of generating seeding patterns to identify important hyperstreamline features. The method is based on anisotropy measurements to optimize the seeding positions and density of hyperstreamlines to reduce visual clutter. Additionally, user can place random distributed seeding points in the tensor field to ensure other minor hyperstreamline features are captured as well. The main advantage of this approach is that the user is not required to have a knowledge of the tensor field in advance.

**KEY WORDS**

Scientific and Mathematical Visualization, Tensor, Hyperstreamline, Seeding.

## 1 Introduction

Visualization of tensor fields is a challenging problem and becomes more common in medical and engineering areas. Original 3D symmetric tensor can be represented by six independent values. Many important features of the tensor fields are described by the eigenvalues and eigenvectors of 3x3 matrices. Due to the multi-variant nature, conventional vector or scalar visualization techniques can not be easily applied to tensor fields. A hyperstreamline technique [1] has been proposed and is useful in visualization of 3D tensor fields. Although hyperstreamlines can show the rich information of 3D tensor structure, few approaches have been able to address the visual clutter or visualization artifacts, most of which comes from the commonly used regular and random seeding.

We describe a new seeding strategy that can place seeds more cleverly to achieve better visualization quality and help user understand the data.

Our anisotropy based seeding approach intends to recover fiber structure in 3D symmetric tensor fields in a more intelligent and efficient way by using anisotropy measurements to generate seeding around the regions with specific anisotropy characteristics. User interactions and feedbacks are also available for our approach to refine the seeding patterns. More seedings can also be applied to the rest of the volume using Poisson sphere distribution to cover the features that might rise from the empty space.

The rest of this paper is organized as follows: Chapter 2 reviews some existing tensor visualization techniques and seeding strategies; Chapter 3 describes how the anisotropy based seeding strategy are applied to hyperstreamlines and implemented; Chapter 4 discusses results and issues of using the seeding strategy; Chapter 5 concludes the paper and identifies additional future works in this area.

## 2 Related Work

There are several visualization techniques for symmetric tensor fields. Among these are arrow plots or hedgehogs [2], ellipsoidal icons [3], tensor glyphs [4], hyperstreamlines [1], tensorlines [5], hyperstreamsurfaces [2], HyperLIC [6] and superquadric tensor glyphs [7]. We review those methods which are relevant to this paper.

Arrow plots or hedgehogs are conventional vector field visualization techniques. Usually they are used for 2D flow and placed on the surface of the flow. They can be directly extended to visualize principal components of 3D real and symmetric tensor fields. This simple approach uses glyphs with short lines with or without arrow heads, usually distributed uniformly across the flow field by regular grid seeding or random seeding. The line orientation indicates the orientation of eigenvectors, while the line length (or line color) is usually used to indicate eigenvalues. Advection is typically not used with hedgehogs and thus only very limited local instantaneous tensor characteristics are shown.

Ellipsoidal icons and tensor glyphs are used to visualize real symmetric tensor fields. Tensor information is encoded with geometric objects. They share the same seedings as hedgehogs and their uses are also limited by their discrete nature.

Hyperstreamlines are generated by constructing a tube or helix structure from the other two eigenvalues and eigenvectors [1]. As a result, hyperstreamlines can fully represent the six values of symmetric tensor fields. When number of hyperstreamlines increases, the visualization loses quality and clutter becomes the key problem since hyperstreamlines have a similar visual representation as streamlines. While the tensor fields determine the direction of hyperstreamlines, it is extremely important to choose seedings carefully.

Tensorlines [5] extends the traditional propagation

methods and stabilize it in isotropic regions. However, it did not address the visual occlusion and clutter issue. Hyperstreamsurfaces use a set of points on a curve to construct a number of hyperstreamlines and then connect them with polygons. They provide some more information but require the user to have some knowledge of the data in order to place the point set at the right position. HyperLIC is a multi-pass approach to generate images that resemble those of LIC to visualize the anisotropy in tensor fields. Superquadric tensor glyphs are used as tensor glyphs in a new way to encode more information and express the property of symmetry.

Among the existing tensor visualization techniques, there is very limited discuss about the seeding problem besides using a regular grid seeding or random seeding. But we will see that it's a key problem in the visualization of 3D tensor fields.

## 3 Methods

In this chapter, we first review tensor theory and visualization of tensor fields using hyperstreamlines. Then our seeding strategy is described in detail.

### 3.1 Tensor Theory

3D symmetric tensor fields are very common in medical and engineering. At each point, a symmetric tensor T can be represented by a 3x3 matrix composed of six independent values:

$$T = \begin{pmatrix} T_{11} & T_{12} & T_{13} \\ T_{12} & T_{22} & T_{23} \\ T_{13} & T_{23} & T_{33} \end{pmatrix} \tag{1}$$

Furthermore, after eigen decomposition, tensor T has unit-length orthogonal eigenvectors $e_1, e_2, e_3$ and three corresponding real eigenvalues $\lambda_1, \lambda_2, \lambda_3$ which satisfy

$$T e_i = \lambda_i e_i, i = 1, 2, 3 \tag{2}$$

$$\lambda_1 \geq \lambda_2 \geq \lambda_3 \tag{3}$$

The original tensor can be reconstructed by

$$T = \begin{pmatrix} e_1 & e_2 & e_3 \end{pmatrix} \begin{pmatrix} \lambda_1 & 0 & 0 \\ 0 & \lambda_2 & 0 \\ 0 & 0 & \lambda_3 \end{pmatrix} \begin{pmatrix} e_1{}^T \\ e_2{}^T \\ e_3{}^T \end{pmatrix} \tag{4}$$

Thus, visualization of a tensor field is fully equivalent to the simultaneous visualization of these three eigenvector fields, with corresponding eigenvalues representing the magnitudes [8][9]. It should be noted that eigenvectors are vectors with sign indeterminacy which asks for additional care in visualization process.

Similar to the critical points in vector fields, in a 3D symmetric tensor field, degenerate points are points where at least two eigenvalues are equal to each other [10]. The integral lines of eigenvectors will cross each other where

degeneracy occurs. Three types of degenerate points can be expressed as

$$\lambda_1 = \lambda_2 > \lambda_3 \tag{5}$$

$$\lambda_1 > \lambda_2 = \lambda_3 \tag{6}$$

$$\lambda_1 = \lambda_2 = \lambda_3 \tag{7}$$

In a diffusion tensor field, fiber structures are very important features, especially in the study of biological tissues from diffusion tensor magnetic resonance imaging datasets. The anisotropic diffusion properties are measured to provide information about the tissue microstructure. Given the eigenvalues defined above, one can define the anisotropy coefficients which correspond to the linear, planar measures

$$c_l = \frac{\lambda_1 - \lambda_2}{\lambda_1 + \lambda_2 + \lambda_3} \tag{8}$$

$$c_p = \frac{2(\lambda_2 - \lambda_3)}{\lambda_1 + \lambda_2 + \lambda_3} \tag{9}$$

and isotropic spherical measure

$$c_s = \frac{3\lambda_3}{\lambda_1 + \lambda_2 + \lambda_3} \tag{10}$$

where

$$c_l + c_p + c_s = 1 \tag{11}$$

An additional coefficient that describes the combined linear and planar anisotropy is the anisotropy index defined as follows:

$$c_a = c_l + c_p = 1 - c_s = \frac{\lambda_1 + \lambda_2 - 3\lambda_3}{\lambda_1 + \lambda_2 + \lambda_3} \tag{12}$$

Based on the movement of water molecules, diffusion tensor in magnetic resonance imaging(DT-MRI) can be used to measure the water anisotropy coefficients in body tissues [11]. Biological tissues can be identified by regions with one or more high anisotropy measurements. It helps the detection of diseases and enables physicians and researchers to better understand and diagnose a wide range of medical conditions.

### 3.2 Hyperstreamlines

The concept of hyperstreamlines [1] is generalized as the propagations of streamlines along one of the eigenvector fields while the stretching of cross section encodes the other two orthogonal eigenvector fields. Hyperstreamlines are called major, medium or minor according to the eigenvector field followed. All the independent values in symmetric tensor fields can be fully represented in this way. Just like streamlines, many hyperstreamlines become a visual clutter that seriously hurt the visualization quality. Thus, in most practices, only very limited number of hyperstreamlines are presented as a direct result. The user is no long able to get a global view and a understanding of the tensor fields. Figure 1 illustrates major eigenvector field for a random generated tensor dataset with (a)15 and (b)400 hyperstreamlines. The visual clutter problem is clearly demonstrated.

(a) 15 hyperstreamlines



(b) 400 hyperstreamlines

Figure 1. Hyperstreamlines of major eigenvector field for a random generated tensor dataset. Color is mapped to major eigenvalue.

## 3.3 Seeding Strategies

There are a number of seeding strategies [12] for generating streamlines. But few can be directly extended to support hyperstreamlines, among those are regular and random seeding. For random seeding, one can use uniform random seeding, regular seeding with jittering, or Poisson disk seeding. Poisson disk seeding in physical space is better suited for curvilinear grids where grid densities may vary a few orders of magnitude within the same data set.

Our seeding strategy starts with selecting one of the anisotropy measurement coefficients from 3.1. High measurement values correspond to anisotropy regions except $c_s$ which actually measures spherical isotropy instead. In practice, biological tissues and fiber structures can be detected by analyzing the linear diffusion $c_l$ or a combination of the linear and planar anisotropy coefficients $c_l$ and $c_p$. Then the fiber structures are traced by the hyperstreamlines that propagate along the principal eigenvector direction.

Once the anisotropy measurement coefficient is chosen, we apply an isosurface extraction algorithm to the scalar field defined by this anisotropy. There are several methods for isosurface extraction that we can choose from, such as brute force method and adaptive partition trees (binary or octree). During this process, one or more isovalues that correspond to high tensor anisotropy are used to generate the surface which identifies anisotropy regions. Figure 2 shows one slice of linear anisotropy field and the extracted isosurface from brain dataset.

For the seeding process, the vertices on the extracted isosurface are used as our seeding template. In addition, a minimum distance separation between these seeding points is enforced to ensure that hyperstreamlines will not get too close to each other. Alternatively, we can place the seeds at the centers of every triangle or polygon on the isosurface. The coordinate calculations are inexpensive by just averaging the coordinates of the vertices for each polygon. Hyperstreamlines are generated from these seeding positions and the significant fiber structures are followed accordingly by tracing major eigenvector field. Optionally, the rest of the space can be filled by placing random seed points with Poisson sphere distribution in case minor tensor field features other than anisotropy specified biological tissues are desired.

Post seeding filtering process can also be applied to achieve better quality. There are various criteria including geometric properties such as length and angle, and tensor field properties other than anisotropy that we will explore in future research.

## 4 Results

We tested our seeding strategy on two diffusion tensor fields from DT-MRI data sets. This new imaging technology was invented to allow physicians and researchers to better understand and diagnose a wide range of medical conditions. By measuring the 3D motion of water
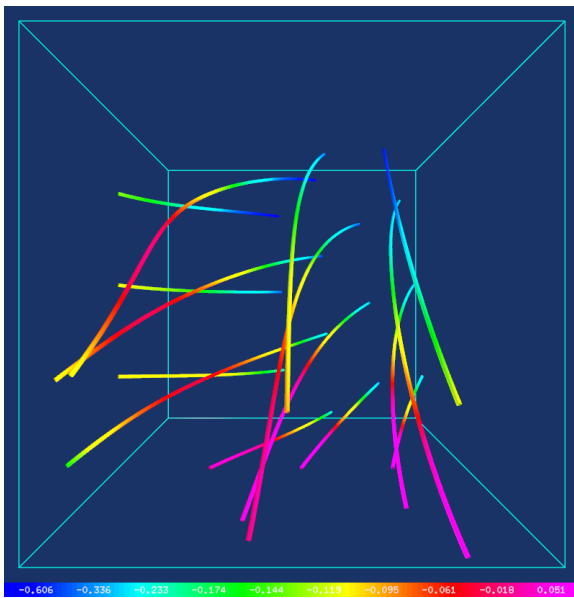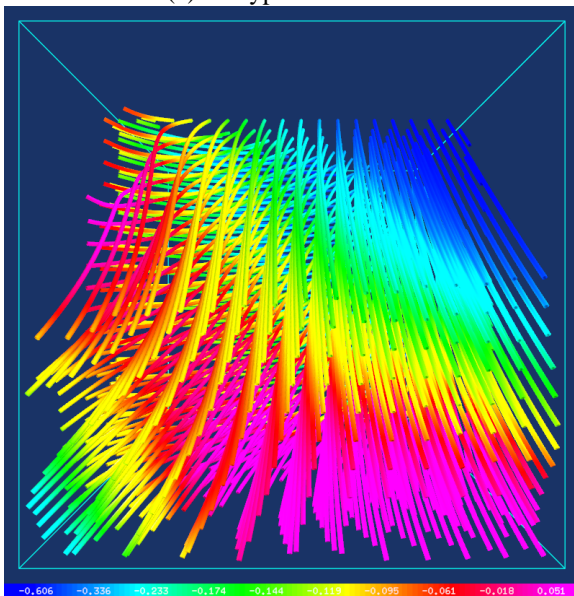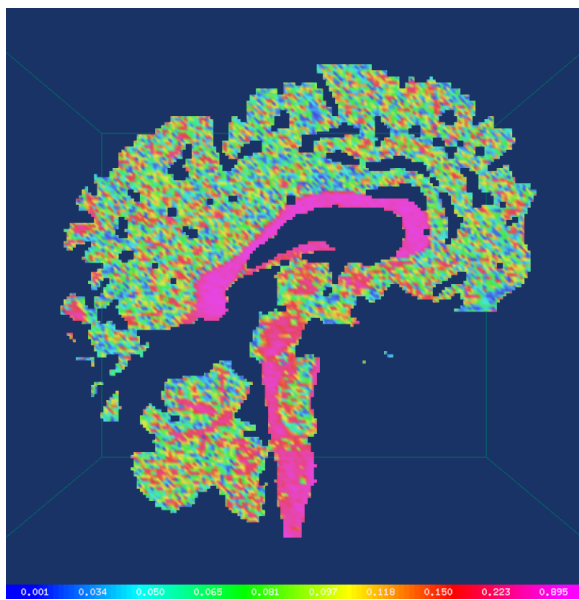
(a) Anisotropy field
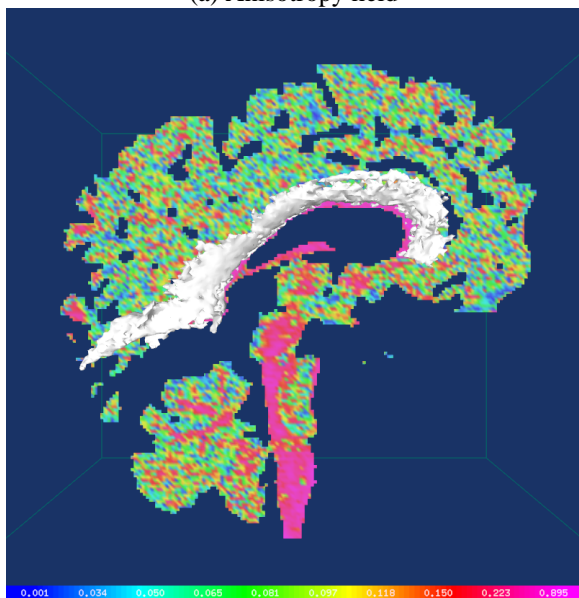


(b) Isosurface(white), largest connected region

Figure 2. Linear anisotropy field of brain dataset and isosurface extracted with an isovalue of 0.5. Color is mapped to linear anisotropy coefficient $c_l$.

molecules within biological tissues, the anisotropic diffusion properties are studied to reveal the fiber structures. We applied our hyperstreamline seeding strategy to a human brain [13][14][15] dataset having 148x190x160 resolution and a human heart [16] dataset which is of 256x256x256 resolution. These data sets are full 3D grids with 3D diffusion tensor information at each point. Figure 3 is an example of visualization using hyperstreamlines generated by random seeding with Poisson sphere distribution. From this figure, it is very difficult for the user to understand the dataset or identify the fiber structures due to visual clutter occlusion. Figure 4, 5 and 6 illustrate the result of this anisotropy based seeding approach when applied to these two diffusion tensor MRI data sets. For the brain dataset, white matter fiber structures are effectively detected by using a linear anisotropy value of 0.5 for the surface extraction. In the heart muscle, the major and median eigenvalues are very close to each other even in the regions corresponding to biological tissues. For this reason, we use the anisotropy combined from linear and planar coefficients. The 0.35 anisotropy value also identifies the heart muscle structure as in figure 6.

In this paper, we use Jacobi's method [17] to compute the eigenvalues and eigenvectors. Jacobi iteration is a reliable method that produces uniformly accurate eigenpairs for a symmetric matrix. Using this method, a solution is guaranteed for all real symmetric matrices.

The hyperstreamline seeding program is written in C++ and uses OpenGL for graphics, FLTK for the graphical user interface and VTK for the isosurface extraction(marching cubes). It was tested on a 1.8 GHz Pentium 4 computer with an ATI Radeon 7500 32MB graphics card and 1GB RAM. It takes approximate one minute for the whole seeding process and hyperstreamlines generation.

## 5    Conclusions and Future Work

In this paper, we present a seeding strategy based on anisotropy measurements for visualizing 3D symmetric tensor data using hyperstreamlines. This approach enables automated generation of seeding templates to achieve a better visualization quality while still having a global view over the whole tensor fields. Its main strength is, the use is not required to have an a priori knowledge of the tensor field. Prior tensor analysis or general information about the tensor topology will be helpful but is not required. Some future directions include: (a) exploring the possibility of extending this anisotropy based approach on tensor fields other than diffusion tensor or symmetric tensor, (b) applying efficient filtering algorithms based on anisotropy or other tensor properties that can further refine the hyperstreamlines, (c) combining tensor topology analysis and tensor property measurements for seeding and clutter reduction purposes.
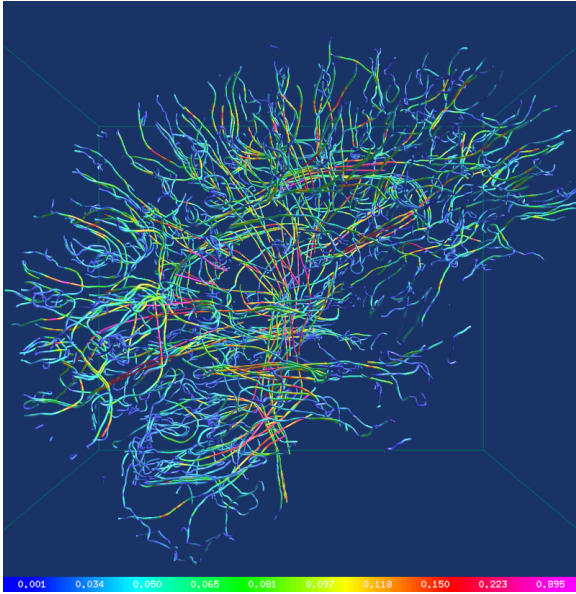
Figure 3. Hyperstreamlines generated from major eigenvector field of human brain diffusion tensor dataset. Random seeding with Poisson sphere distribution. Color is mapped to linear anisotropy $c_l$. 500 hyperstreamlines.
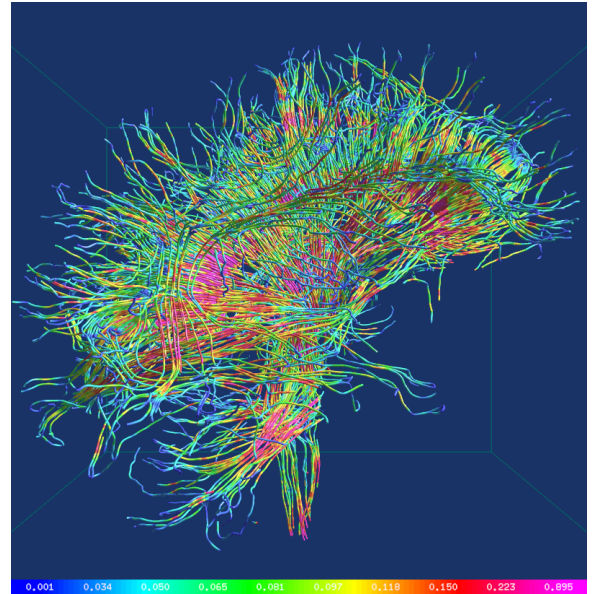


Figure 5. Hyperstreamlines generated from major eigenvector field of human brain diffusion tensor dataset. A linear anisotropy measurement value $c_l = 0.5$ is used to extract the isosurface and form the seeding template. Color is mapped to $c_l$. 1200 hyperstreamlines.
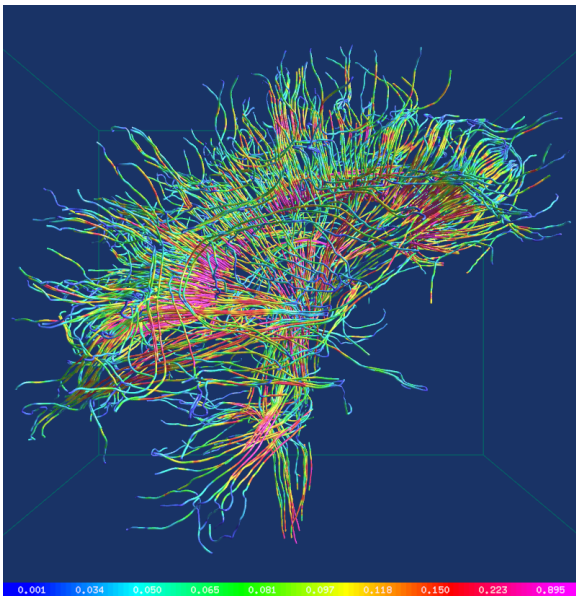


Figure 4. Hyperstreamlines generated from major eigenvector field of human brain diffusion tensor dataset. A linear anisotropy measurement value $c_l = 0.5$ is used to extract the isosurface and form the seeding template. Color is mapped to linear anisotropy coefficient $c_l$. 500 hyperstreamlines.
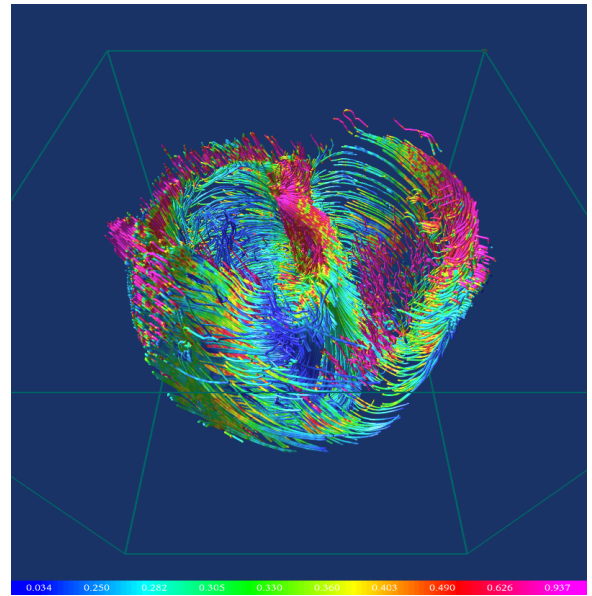


Figure 6. Hyperstreamlines generated from major eigenvector field of human heart diffusion tensor dataset. A sum of linear and planar measurement value $c_a = 0.35$ is used to extract the isosurface and form the seeding template. Color is mapped to anisotropy coefficient $c_a$. 800 hyperstreamlines.

## References

[1] Thierry Delmarcelle and Lambertus Hesselink, Visualizing Second-Order Tensor Fields with Hyperstreamlines, *IEEE Computer Graphics and Applications 13(4)*, July 1993, 25-33.

[2] Boris Jeremić, Gerik Scheuermann, Jan Frey, Zhaohui Yang, Bernd Hamann, Kenneth I. Joy and Hans Hagen, Tensor Visualizations in Computational Geomechanics, *International Journal for Numerical and Analytical Methods in Geomechanics 26*, 2002, 925-944.

[3] C. Upson, R. Wolff, R. Weinberg and D. Kerlich, Two and Three Dimensional Visualization Workshop, *SIGGRAPH*, 1989, Course Number 19.

[4] R.B. Haber, Visualization Techniques for Engineering Mechanics, *Computing Systems in Engineering, 1(1)*, 1990, 37-50.

[5] David Weinstein, Gordon Kindlmann and Eric Lundberg, Tensorlines: Advection-Diffusion Based Propagation Through Diffusion Tensor Fields, *Proceedings of Visualization*, 1999, 249-253.

[6] Xiaoqiang Zheng and Alex Pang, HyperLIC, *Proceedings IEEE Visualization*, 2003, 33.

[7] Gordon Kindlmann, Superquadric Tensor Glyphs, *Proceedings IEEE TVCG/EG Symposium on Visualization*, 2004.

[8] Thierry Delmarcelle and Lambertus Hesselink, Visualization of Second Order Tensor Fields and Matrix Data, *IEEE Visualization Proceedings*, 1992, 316-322.

[9] Thierry Delmarcelle and Lambertus Hesselink, The topology of Symmetric, Second-Order Tensor Fields, *IEEE Visualization Proceedings*, 1994, 140-147.

[10] Yingmei Lavin, Yuval Levy and Lambertus Hesselink, Singularities in Nonuniform Tensor Fields, *Proceedings of Visualization*, 1997, 59-66.

[11] E. Hsu and C. Henriquez, Myocardial Fiber Orientation Mapping Using Reduced Encoding Diffusion Tensor Imaging, *Journal of Cardiovascular Magnetic resonance 3*, 2001, 339-347.

[12] Vivek Verma, David Kao and Alex Pang, A Flow-guided Streamline Seeding Strategy, *Proceedings IEEE Visualization*, 2000, 163-170.

[13] Gordon Kindlmann and David Weinstein, Hue-Balls and Lit-Tensors for Direct Volume Rendering of Diffusion Tensor Fields, *IEEE Visualization Proceedings*, 1999, 183-189.

[14] Leonid Zhukov and Alan H. Barr, Oriented Tensor Reconstruction: Tracing Neural Pathways from Diffusion Tensor MRI, *IEEE Visualization Proceedings*, 2002, 387-394.

[15] Song Zhang, Çagatay Demiralp and David H. Laidlaw, Visualizing Diffusion Tensor MR Images Using Streamtubes and Streamsurfaces, *IEEE Transactions on Visualization and Computer Graphics 9(4)*, 2003, 454-462.

[16] Leonid Zhukov and Alan H. Barr, Heart-Muscle Fiber Reconstruction from Diffusion Tensor MRI, *Proceedings IEEE Visualization*, 2003.

[17] William H. Press, Brian P. Flannery, Saul A. Teukolsky and William T. Vetterling, *Numerical Recipes in C : The Art of Scientific Computing* (Cambridge University Press. 2nd edition, October 30, 1992).